Structural Engineering and Mechanics, Vol. 25, No. 6 (2007) 753-765

DOI: http://dx.doi.org/10.12989/sem.2007.25.6.753

Response of dynamic interlaminar stresses in laminated plates under free vibration and thermal load

S.Q. Zhu†, X. Chen‡ and X. Wang‡†

School of Naval Architecture, Ocean and Civil Engineering, Shanghai Jiao Tong University, Shanghai 200240, P.R. China

(Received February 23, 2006, Accepted October 11, 2006)

Abstract. The response histories and distribution of dynamic interlaminar stresses in composite laminated plates under free vibration and thermal load is studied based on a thermoelastodynamic differential equations. The stacking sequence of the laminated plates may be arbitrary. The temperature change is considered as a linear function of coordinates in planes of each layer. The dynamic mode of displacements is considered as triangle series. The in-plane stresses are calculated by using geometric equations and generalized Hooke's law. The interlaminar stresses are evaluated by integrating the 3-D equations of equilibrium, and utilizing given boundary conditions and continuity conditions of stresses between layers. The response histories and distribution of interlaminar stress under thermal load are presented for various vibration modes and stacking sequence. The theoretical analyses and results are of certain significance in practical engineering application.

Keywords: composite laminated plates; dynamic interlaminar stresses; thermal environment.

1. Introduction

Composite laminated structures are being increasingly used in aerospace and aeronautical area. These structures are often subjected to combinations of dynamic mechanical loads and thermal loading. One of the main causes to failure of composite laminated structures is delamination damage, which is significantly derived from interlaminar stresses. Previous research was mainly limited in the interlaminar stress distributions in laminated structure under static load, while response histories and distribution of dynamic interlaminar stresses was seldom mentioned (Reddy 1996). Several scholars (Carvalho and Guedes Soares 1996, Ganapathy and Rao 1997, Babeshko 1996) presented theoretical and numerical methods to predict the interlaminar stresses in composite laminated plates. A simple iterative method (Makeev and Armanios 1994) was applied to evaluate interlaminar stresses in composite laminated subjected to axial tension and torsion loads. Some other methods (Becker, Peng and Neuser 1999, Cho and Yoon 1999, Yong and Cho 1995, Di and Ramm 1993) were presented to calculate interlaminar stresses at various positions in laminates. The interlaminar stresses in laminated plates subjected to vibration were analyzed in reference (Jane and

† Master
‡ Master
‡† Professor, Ph.D., Corresponding author, E-mail: xwang@sjtu.edu.cn

Hong 2000), but in the paper, the effect of thermal load was not taken into account. Thermal stresses of composite laminated structures studied in papers (Verijenko and Tauchert 1999, Savchenko 1995, Chandrashekhara and Bhimaraddi 1994, Ding and Tang 1999, Zhang and Liu 1992) are also limited in static problems. The papers (Jianqiao and Soldatos 1996, Messina and Soldatos 2002) reported the results of an investigation into free vibration analysis and continuity interlaminar stresses in laminated composite based on higher order theories.

In this paper, the response histories and distribution of interlaminar stresses in rectangular laminated plates with simply supported edges, subjected to free vibration and in thermal environment is studied in some depth. The temperature change is considered as a linear function of coordinates in planes of each layer. A theoretical solution to predict the interlaminar stresses in composite laminated plates subjected to free vibration and thermal load is presented for considering various vibration modes and stacking sequence. Some numerical examples and results on the problem are also presented and discussed.

2. Govering equation

The structure of rectangular orthotropic laminated plates with simply supported edges is shown in Fig. 1. The relationship between stresses and strains in plane is expressed as (Tsai and Hahn 1980)

$$\begin{Bmatrix} \sigma_x^{(k)} \\ \sigma_y^{(k)} \\ \tau_{xy}^{(k)} \end{Bmatrix} = \begin{bmatrix} \overline{Q}_{11}^{(k)} & \overline{Q}_{12}^{(k)} & \overline{Q}_{16}^{(k)} \\ \overline{Q}_{12}^{(k)} & \overline{Q}_{22}^{(k)} & \overline{Q}_{26}^{(k)} \\ \overline{Q}_{16}^{(k)} & \overline{Q}_{26}^{(k)} & \overline{Q}_{66}^{(k)} \end{bmatrix} \left(\begin{Bmatrix} \varepsilon_x^{(k)} \\ \varepsilon_y^{(k)} \\ \gamma_{xy}^{(k)} \end{Bmatrix} - \begin{Bmatrix} \alpha_x \\ \alpha_y \\ \alpha_{xy} \end{Bmatrix} \Delta T^{(k)} \right) \tag{1}$$

where $\{\sigma_i^k\}$, $\{\varepsilon_i^k\}$ and $\Delta T^k(x, y)$ represent, respectively, the stress, the strain and the temperature change of the kth layer. $[\overline{Q}_{ij}^{(k)}]$ and $\{\alpha_i^k\}_{i = x, y, xy}$ represent, respectively, the bias axial stiffness coefficient and the bias axial thermal expansion coefficient of a single layer in the geometrical coordinate (x, y, z) system, and are, respectively, expressed as

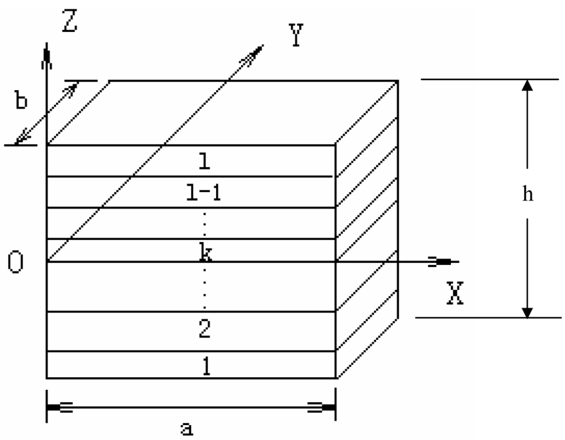

Fig. 1 The structure of rectangular orthotropic laminated plates with simply supported edges

$$[\bar{Q}_{ij}^{(k)}] = \begin{bmatrix} c^2 & s^2 & -2cs \\ s^2 & c^2 & 2cs \\ cs & -cs & c^2-s^2 \end{bmatrix} \begin{bmatrix} Q_{11}^k & Q_{12}^k & 0 \\ Q_{12}^k & Q_{22}^k & 0 \\ 0 & 0 & Q_{66}^k \end{bmatrix} \begin{bmatrix} c^2 & s^2 & -cs \\ s^2 & c^2 & cs \\ 2cs & -2cs & c^2-s^2 \end{bmatrix} \tag{2a}$$

$$\{\alpha_i^k\}_{i=x,y,xy} = \begin{bmatrix} c^2 & s^2 \\ s^2 & c^2 \\ 2cs & -2cs \end{bmatrix} \begin{Bmatrix} \alpha_1 \\ \alpha_2 \end{Bmatrix} \tag{2b}$$

where α_1 and α_2 are, respectively, the thermal expansion coefficient measured in the fiber and transverse directions of a single player in the material main axis (1-2)

$$Q_{11} = \frac{E_{11}}{1-\nu_{12}\nu_{21}}, \quad Q_{22} = \frac{E_{22}}{1-\nu_{12}\nu_{21}}, \quad Q_{12} = \frac{E_{21}E_{11}}{1-\nu_{12}\nu_{21}}, \quad Q_{66} = G_{12} \tag{2c}$$

and

$$c = \cos\theta \quad \text{and} \quad s = \sin\theta \tag{2d}$$

where θ is the lamination angle with respect to the plate x-axis.

Based on a micro-mechanical model of the laminate (Bowles and Tompkins 1989), the thermal expansion coefficients in the longitudinal and transverse directions of fiber are expressed as

$$\alpha_1 = \frac{V_f E_f \alpha_f + V_m E_m \alpha_m}{V_f E_f + V_m E_m} \tag{3a}$$

$$\alpha_2 = (1+\nu_f)V_f\alpha_f + (1+\nu_m)V_m\alpha_m - \nu_{12}\alpha_1 \tag{3b}$$

where α_f and α_m are thermal expansion coefficients of the fiber and matrix, respectively.

In the above formula, V_f and V_m are the fiber and matrix volume fractions and are related by

$$V_f + V_m = 1 \tag{4}$$

and E_f, G_f and ν_f are, respectively, the Young's modulus, shear modulus and Poisson's ratio of the fiber and E_m, G_m and ν_m are the corresponding properties for the matrix. Thus, the material properties of lamina are expressed as

$$E_{11} = V_f E_f + V_m E_m \tag{5a}$$

$$\frac{1}{E_{22}} = \frac{V_f}{E_f} + \frac{V_m}{E_m} - V_f V_m \frac{\nu_f^2 E_m/E_f + \nu_m^2 E_f/E_m - 2\nu_f\nu_m}{V_f E_f + V_m E_m} \tag{5b}$$

$$G_{12} = \frac{V_f G_m + V_m G_f}{G_f G_m}, \quad \nu_{12} = V_f\nu_f + V_m\nu_m, \quad \nu_{21} = \frac{E_2}{E_1}\nu_{12} \tag{5c}$$

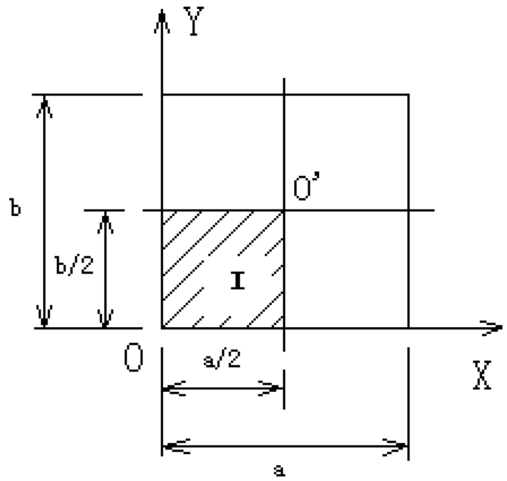

Fig. 2 The plane structure of the laminated plates with simply supported edges. I represents 1/4 symmetry region of the laminated plates

The study is based on 1/4 of the plane area according to symmetry of laminated plates. Suppose the variation of the temperature at the center of $x-y$ plane shown in Fig. 2 is ΔT_0, and $\Delta T^{(k)}(x,y)$ (the temperature variation at any position) is linear function of ΔT_0 related to x and y as follows

$$\Delta T^{(k)}(x,y) = \Delta T_0(x+y+1) \tag{6}$$

The geometric equation is given by

$$\varepsilon_{ij} = \frac{1}{2}(u_{i,j}+u_{j,i}) \tag{7a}$$

Form Eq. (7a), the displacement expressions is represented as

$$u=-z\frac{\partial w}{\partial x},\quad v=-z\frac{\partial w}{\partial y},\quad w=w(x,y,t) \tag{7b}$$

Substituting Eq. (7) into Eq. (1), the plane stresses in the k layer of laminated plates in thermal environment can be rewritten as

$$\begin{Bmatrix}\sigma_x^{(k)}\\ \sigma_y^{(k)}\\ \tau_{xy}^{(k)}\end{Bmatrix} = \begin{bmatrix}\overline{Q}_{11}^{(k)} & \overline{Q}_{12}^{(k)} & \overline{Q}_{16}^{(k)}\\ \overline{Q}_{12}^{(k)} & \overline{Q}_{22}^{(k)} & \overline{Q}_{26}^{(k)}\\ \overline{Q}_{16}^{(k)} & \overline{Q}_{26}^{(k)} & \overline{Q}_{66}^{(k)}\end{bmatrix}\left(\begin{Bmatrix}-z\dfrac{\partial^2 w}{\partial x^2}\\ -z\dfrac{\partial^2 w}{\partial y^2}\\ -2z\dfrac{\partial^2 w}{\partial x\partial y}\end{Bmatrix} - \begin{Bmatrix}\alpha_x\\ \alpha_y\\ \alpha_{xy}\end{Bmatrix}\Delta T_0(x+y+1)\right) \tag{8}$$

3. Response of dynamic interlaminar stresses

For the kth layer of laminated plates, the differential equations of dynamic equilibrium without considering inertial forces f_i is represented as

$$\sigma_{ij,j}^{(k)} = \rho^{(k)}\frac{\partial^2 u_i}{\partial t^2}, \quad (i,j = 1,2,3) \tag{9}$$

Integrating for Eq. (9) over z, dynamic interlaminar stresses are represented as

$$\tau_{xz}^{(k)} = \int\left(\rho^{(k)}\frac{\partial^2 u^{(k)}}{\partial t^2} - \frac{\partial \sigma_x^{(k)}}{\partial x} - \frac{\partial \tau_{xy}^{(k)}}{\partial y}\right)dz \tag{10a}$$

$$\tau_{yz}^{(k)} = \int\left(\rho^{(k)}\frac{\partial^2 v^{(k)}}{\partial t^2} - \frac{\partial \tau_{xy}^{(k)}}{\partial x} - \frac{\partial \sigma_y^{(k)}}{\partial y}\right)dz \tag{10b}$$

$$\sigma_z^{(k)} = \int\left(\rho^{(k)}\frac{\partial^2 w^{(k)}}{\partial t^2} - \frac{\partial \tau_{xz}^{(k)}}{\partial x} - \frac{\partial \tau_{yz}^{(k)}}{\partial y}\right)dz \tag{10c}$$

The boundary conditions of laminated plates with simply supported boundary are expressed as

$$x = 0, a: \quad W = \frac{\partial^2 W}{\partial x^2} = 0; \quad y = 0, b: \quad W = \frac{\partial^2 W}{\partial y^2} = 0 \tag{11}$$

The mode function of free vibration of the laminated plates with simply supported boundary (11) may be expressed as

$$W(x,y) = \sin\frac{m\pi x}{a}\sin\frac{n\pi y}{b} \tag{12}$$

and the corresponding displacement mode is written as

$$w(x,y,t) = W(x,y)\sin(\omega_{mn}t) \tag{13}$$

where ω_{mn} expresses the nature frequency of free vibration of laminated plates, which is easily obtained based on the corresponding stacking sequence of laminated plates, m and n are, respectively, wave numbers of vibration along x and y directions.

Substituting Eq. (13) into Eq. (7b), yields

$$u = -z\frac{m\pi}{a}\cos\frac{m\pi x}{a}\sin\frac{n\pi y}{b}\sin\omega_{mn}t \tag{14a}$$

$$v = -z\frac{n\pi}{b}\sin\frac{m\pi x}{a}\cos\frac{n\pi y}{b}\sin\omega_{mn}t \tag{14b}$$

$$w = \sin\frac{m\pi x}{a}\sin\frac{n\pi y}{b}\sin\omega_{mn}t \tag{14c}$$

Substituting Eqs. (8) and (14) into (10) and integrating over z, we have

$$\begin{aligned}\tau_{xz}^{(k)} &= \frac{z^2}{2}\left\{\left[\rho^{(k)}\omega_{mn}^2\frac{m\pi}{a} - \overline{Q}_{11}^{(k)}\frac{m^3\pi^3}{a} - (\overline{Q}_{12}^{(k)} + 2\overline{Q}_{66}^{(k)})\frac{mn^2\pi^3}{ab^2}\right]\times\right.\\ &\left.\cos\frac{m\pi x}{a}\sin\frac{n\pi y}{b} - \left(3\overline{Q}_{16}^{(k)}\frac{m^2n\pi^3}{a^2b} + \overline{Q}_{26}^{(k)}\frac{n^3\pi^3}{b^3}\right)\sin\frac{m\pi x}{a}\cos\frac{n\pi y}{b}\right\}\sin\omega_{mn}t\\ &+ z\Delta T_0[(\overline{Q}_{11}^k + \overline{Q}_{16}^k)\alpha_x^k + (\overline{Q}_{12}^k + \overline{Q}_{26}^k)\alpha_y^k + (\overline{Q}_{16}^k + \overline{Q}_{66}^k)\alpha_{xy}^k] + f^{(k)}(x,y)\\ &= \tau_{xz0}^k(x,y,z) + f^k(x,y)\end{aligned} \tag{15a}$$

$$\begin{aligned}\tau_{yz}^{(k)} &= \frac{z^2}{2}\left\{\left[\rho^{(k)}\omega_{mn}^2\frac{n\pi}{b} - \overline{Q}_{22}^{(k)}\frac{n^3\pi^3}{b^3} - (\overline{Q}_{12}^{(k)} + 2\overline{Q}_{66}^{(k)})\frac{m^2n\pi^3}{a^2b}\right]\times\right.\\ &\left.\sin\frac{m\pi x}{a}\cos\frac{n\pi y}{b} - \left(\overline{Q}_{16}^{(k)}\frac{m^3\pi^3}{a^3} + 3\overline{Q}_{26}^{(k)}\frac{mn^2\pi^3}{ab^2}\right)\cos\frac{m\pi x}{a}\sin\frac{n\pi y}{b}\right\}\sin\omega_{mn}t\\ &+ z\Delta T_0[(\overline{Q}_{12}^k + \overline{Q}_{16}^k)\alpha_x^k + (\overline{Q}_{22}^k + \overline{Q}_{26}^k)\alpha_y^k + (\overline{Q}_{26}^k + \overline{Q}_{66}^k)\alpha_{xy}^k] + g^{(k)}(x,y)\\ &= \tau_{yz0}^k(x,y,z) + g^k(x,y)\end{aligned} \tag{15b}$$

$$\begin{aligned}\sigma_z^{(k)} &= \left\{-z\rho^{(k)}\omega_{mn}^2 + \frac{z^3}{6}\left[\rho^{(k)}\omega_{mn}^2\left(\frac{m^2\pi^2}{a^2} + \frac{n^2\pi^2}{b^2}\right) - 2(\overline{Q}_{12}^{(k)} + 2\overline{Q}_{66}^{(k)})\times\right.\right.\\ &\left.\left.\frac{m^2n^2\pi^4}{a^2b^2} - \overline{Q}_{11}^{(k)}\frac{m^4\pi^4}{a^4} - \overline{Q}_{22}^{(k)}\frac{n^4\pi^4}{b^4}\right\}\right]\sin\frac{m\pi x}{a}\sin\frac{n\pi y}{b}\sin\omega_{mn}t\\ &+ \frac{2z^3}{3}\left(\overline{Q}_{16}^{(k)}\frac{m^3n\pi^4}{a^3b} + \overline{Q}_{26}^{(k)}\frac{mn^3\pi^4}{ab^3}\right)\cos\frac{m\pi x}{a}\cos\frac{n\pi y}{b}\sin\omega_{mn}t\\ &- z\left[\frac{\partial f^{(k)}(x,y)}{\partial x} + \frac{\partial g^{(k)}(x,y)}{\partial y}\right] + h^{(k)}(x,y)\\ &= \sigma_{z0}^k(x,y,z) + h^k(x,y)\end{aligned} \tag{15c}$$

where $\tau_{xz0}^k(x,y,z)$, $\tau_{yz0}^k(x,y,z)$ and $\sigma_z^k(x,y,z)$ are the known functions, f^k, g^k, h^k are undetermined functions related to x and y, which is determined by utilizing the upper and bottom surfaces conditions of laminated plates and the continuity conditions of interlaminar stresses between layers as follows stresses in the upper and bottom of the laminated plate

$$\tau_{xz}^l = \tau_{yz}^l = \sigma_z^l = 0, \quad (z = z_l) \tag{16a}$$

$$\tau_{xz}^1 = \tau_{yz}^1 = \sigma_z^1 = 0, \quad (z = z_1 - h_1) \tag{16b}$$

continuity conditions of interlaminar stresses between layers

$$\tau_{xz}^k = \tau_{xz}^{k+1}, \quad \tau_{yz}^k = \tau_{yz}^{k+1}, \quad \sigma_z^k = \sigma_z^{k+1}; \quad z = z_k;\ k = 1, 2, \ldots, l-1 \tag{16c}$$

Substituting Eq. (15) into Eq. (16a), gives

$$
\begin{aligned}
f^{l}(x,y) &= -\tau^{l}_{xz0}(x,y,z_l)\\
g^{l}(x,y) &= -\tau^{l}_{yz0}(x,y,z_l)\\
h^{l}(x,y) &= -\sigma^{l}_{z0}(x,y,z_l)
\end{aligned} \tag{17}
$$

Substituting Eq. (17) into Eq. (15), the stress out-plane of the *l*th layer can be determined as

$$
\begin{aligned}
\tau^{l}_{xz} &= \tau^{l}_{xz0}(x,y,z) - \tau^{l}_{xz0}(x,y,z_l)\\
\tau^{l}_{yz} &= \tau^{l}_{yz0}(x,y,z) - \tau^{l}_{yz0}(x,y,z_l)\\
\sigma^{l}_{z} &= \sigma^{l}_{z0}(x,y,z) - \sigma^{l}_{z0}(x,y,z_l)
\end{aligned} \tag{18}
$$

Utilizing the continuity condition (16c) of interlaminar stresses between the *l*th layer and the $(l-1)$th layer, the undetermined function of the $(l-1)$th layer can be given by

$$
\begin{aligned}
f^{l-1}(x,y) &= \tau^{l}_{xz}(x,y,z_{l-1}) - \tau^{l-1}_{xz0}(x,y,z_{l-1})\\
g^{l-1}(x,y) &= \tau^{l}_{yz}(x,y,z_{l-1}) - \tau^{l-1}_{yz0}(x,y,z_{l-1})\\
h^{l-1}(x,y) &= \sigma^{l}_{z}(x,y,z_{l-1}) - \sigma^{l-1}_{z0}(x,y,z_{l-1})
\end{aligned} \tag{19}
$$

Similar to the above method, the undetermined function of the *k*th layer is expressed as

$$
\begin{aligned}
f^{k}(x,y) &= \tau^{k+1}_{xz}(x,y,z_k) - \tau^{k}_{xz0}(x,y,z_k)\\
g^{k}(x,y) &= \tau^{k+1}_{yz}(x,y,z_k) - \tau^{k}_{yz0}(x,y,z_k)\\
h^{k}(x,y) &= \sigma^{k+1}_{z}(x,y,z_k) - \sigma^{k}_{z0}(x,y,z_k),\quad k = l-2,\ \ldots,\ 1
\end{aligned} \tag{20}
$$

Thus, substituting $z = z_k$, $(k = l-1, l-2, \ldots, 1)$ into Eq.(15) yields the dynamic interlaminar stress between the *k*th layer and the $(k-1)$th layer which is expressed as

$$
\begin{aligned}
\tau^{k\sim k-1}_{xz} = \frac{z_k^2}{2}\Bigg\{&\left[\rho^k\omega^2_{mn}\frac{m\pi}{a} - \overline{Q}^k_{11}\frac{m^3\pi^3}{a^3} - (\overline{Q}^k_{12} + 2\overline{Q}^k_{66})\frac{mn^2\pi^3}{ab^2}\right]\times\\
&\cos\frac{m\pi x}{a}\sin\frac{n\pi y}{b} - \left(3\overline{Q}^k_{16}\frac{m^2 n\pi^3}{a^2 b} + \overline{Q}^k_{26}\frac{n^3\pi^3}{b^3}\right)\sin\frac{m\pi x}{a}\cos\frac{n\pi y}{b}\Bigg\}\sin\omega_{mn}t\\
&+ z\Delta T_0[(\overline{Q}^k_{11} + \overline{Q}^k_{16})\alpha^k_x + (\overline{Q}^k_{12} + \overline{Q}^k_{26})\alpha^k_y + (\overline{Q}^k_{16} + \overline{Q}^k_{66})\alpha^k_{xy}] + f^k(x,y)
\end{aligned}
$$

$$\tau_{yz}^{k\sim k-1} = \frac{z_k^2}{2}\left\{\left[\rho^k\omega_{mn}^2\frac{n\pi}{b} - \overline{Q}_{22}^k\frac{n^3\pi^3}{b^3} - (\overline{Q}_{12}^k + 2\overline{Q}_{66}^k)\frac{m^2n\pi^3}{a^2b}\right]\times\right.$$

$$\left.\sin\frac{m\pi x}{a}\cos\frac{n\pi y}{b} - \left(\overline{Q}_{16}^k\frac{m^3\pi^3}{a^3} + 3\overline{Q}_{26}^k\frac{mn^2\pi^3}{ab^2}\right)\cos\frac{m\pi x}{a}\sin\frac{n\pi y}{b}\right\}\sin\omega_{mn}t$$

$$+ z\Delta T_0[(\overline{Q}_{12}^k + \overline{Q}_{16}^k)\alpha_x^k + (\overline{Q}_{22}^k + \overline{Q}_{26}^k)\alpha_y^k + (\overline{Q}_{26}^k + \overline{Q}_{66}^k)\alpha_{xy}^k] + g^k(x,y)$$

$$\sigma_z^{k\sim k-1} = \left\{-z_k\rho^k\omega_{mn}^2 + \frac{z_k^3}{6}\left[\rho^k\omega_{mn}^2\left(\frac{m^2\pi^2}{a^2} + \frac{n^2\pi^2}{b^2}\right) - 2(\overline{Q}_{12}^k + 2\overline{Q}_{66}^k)\times\right.\right.$$

$$\left.\left.\frac{m^2n^2\pi^4}{a^2b^2} - \overline{Q}_{11}^k\frac{m^4\pi^4}{a^4} - \overline{Q}_{22}^k\frac{n^4\pi^4}{b^4}\right\}\right]\sin\frac{m\pi x}{a}\sin\frac{n\pi y}{b}\sin\omega_{mn}t$$

$$+ \frac{2z_k^3}{3}\left(\overline{Q}_{16}^k\frac{m^3n\pi^4}{a^3b} + \overline{Q}_{26}^k\frac{mn^3\pi^4}{ab^3}\right)\cos\frac{m\pi x}{a}\cos\frac{n\pi y}{b}\sin\omega_{mn}t$$

$$- z_k\left[\frac{\partial f^k(x,y)}{\partial x} + \frac{\partial g^k(x,y)}{\partial y}\right] + h^k(x,y) \tag{21}$$

4. Numerical results and discussions

To study the effects of temperature, humidity and electric fields on the response histories of dynamic interlaminar stresses in laminated plates, several numerical examples were solved for different stacking sequence laminated plates. Graphite/epoxy composite material was selected for the plates in the present examples. The material properties adopted are (Adams and Miller 1977)

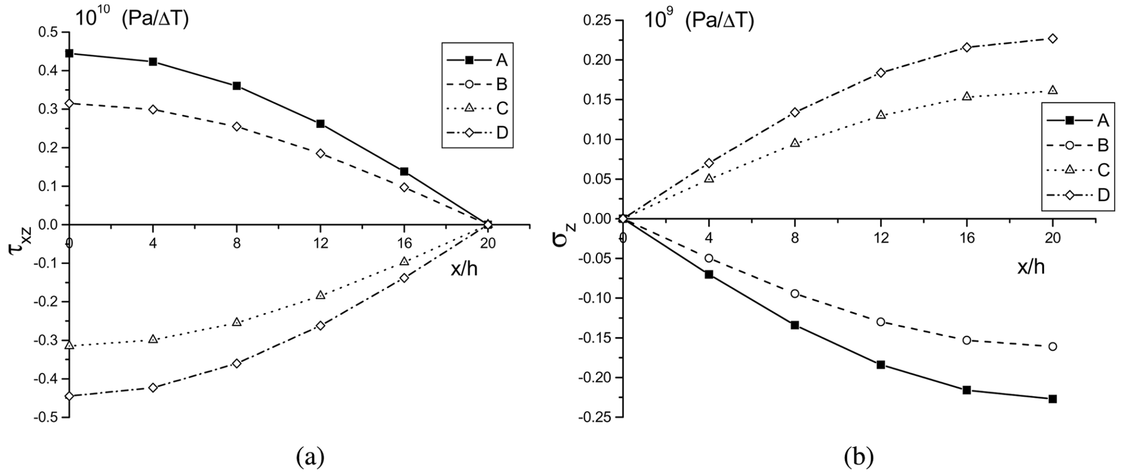

Fig. 3 (a,b) The response histories and distribution of interlaminar stress in laminated plates with the stacking sequence $[0^o/90^o]_s$, under vibration mode of $\varpi_{11} = 138$ rad/s. The curves A, B, C and D represent, respectively, the interlaminar stresses at times $t = 0.5\varpi_{11}\pi$, $t = 0.75\varpi_{11}\pi$, $t = 1.25\varpi_{11}\pi$ and $t = 1.5\varpi_{11}\pi$

$E_f = 230$ (GPa), $G_f = 9$ (GPa), $v_f = 0.203$, $\alpha_f = -0.54 \times 10^{-6}/^{\circ}\mathrm{C}$, $\rho_f = 1750\ \mathrm{kg/m^3}$, $v_m = 0.34$, $\alpha_m = 45 \times 10^{-6}/^{\circ}\mathrm{C}$, $\rho_m = 1200\ \mathrm{kg/m^3}$ and $E_m = 3.51$ (GPa). Here, the analysis is equally applicable to other types of composite materials. For these examples, the thickness h_s of single fibre reinforced layer is taken as 2.5 mm. The lengths of both sides on laminated plates are, respectively, $a = b = 40\ h = 400\ \mathrm{mm}$. $h = lh_s$ express the thickness of the laminated plates. $\Delta T(^{\circ}\mathrm{C})$ represents temperature change. The interlaminar stresses in the interface $z = h_s$ and at positions $y = 20\ h$ are calculated as follows.

Fig. 3 shows the distribution of interlaminar stresses τ_{xz} and σ_z in the laminar plates with stacking sequence $[0^{\circ}/90^{\circ}]_s$ along the x-axis, under the vibration mode for $\varpi_{11} = 138$ rad/s. The results

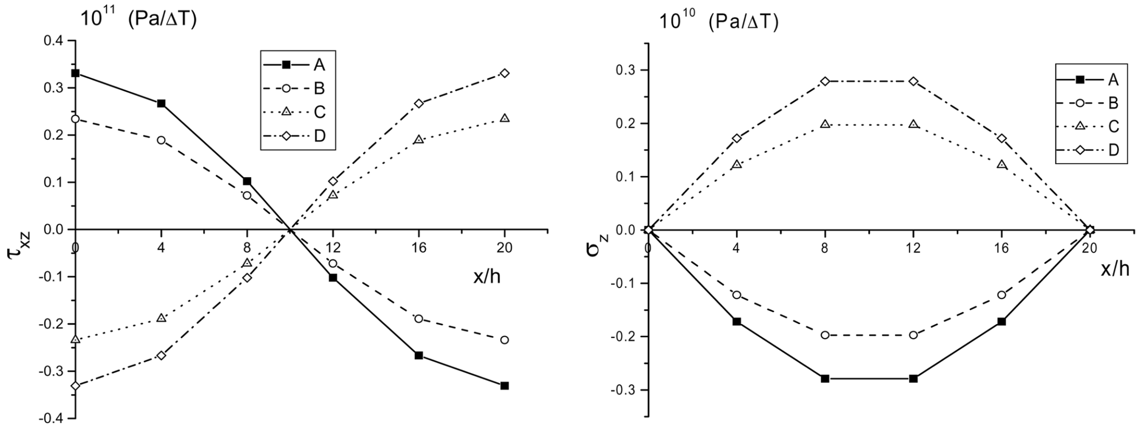

(a) (b)

Fig. 4 (a,b) The response histories and distribution of interlaminar stress in laminated plates with the stacking sequence $[0^{\circ}/90^{\circ}]_s$, under vibration mode of $\varpi_{21} = 469$ rad/s. The curves A, B, C and D represent, respectively, the interlaminar stresses at times $t = 0.5\varpi_{21}\pi$, $t = 0.75\varpi_{21}\pi$, $t = 1.25\varpi_{21}\pi$ and $t = 1.5\varpi_{21}\pi$

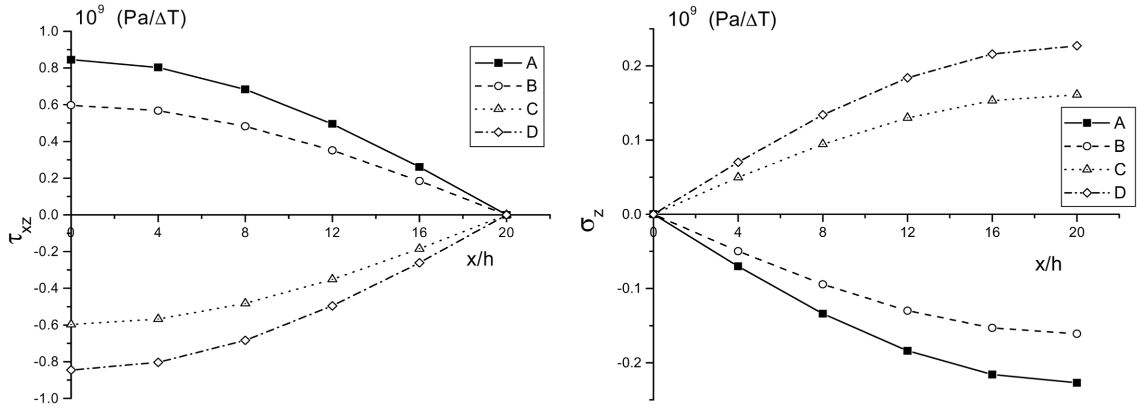

(a) (b)

Fig. 5 (a,b) The response histories and distribution of interlaminar stress in laminated plates with the stacking sequence $[90^{\circ}/0^{\circ}]_s$, under vibration mode of $\varpi_{11} = 138$ rad/s. The curves A, B, C and D represent, respectively, the interlaminar stresses at times $t = 0.5\varpi_{11}\pi$, $t = 0.75\varpi_{11}\pi$, $t = 1.25\varpi_{11}\pi$ and $t = 1.5\varpi_{11}\pi$

indicate that τ_{xz} is decreasing along with the x-axis, while σ_z is on the contrary. Fig. 4 shows the distribution of interlaminar stresses τ_{xz} and σ_z in the laminar plates with stacking sequence $[0^o/90^o]_s$ along x-axis, under the vibration mode for $\varpi_{21} = 469$ rad/s. The results indicate that τ_{xz} arrives at the minimum at $x/h = 10$, where σ_z reached the maximum.

Fig. 5 shows the distribution of interlaminar stresses τ_{xz} and σ_z in the laminar plates with stacking sequence $[90^o/0^o]_s$ along x-axis, under the vibration mode for $\varpi_{11} = 138$ rad/s. The results indicate that τ_{xz} is decreasing along the x-axis, while σ_z is on the contrary. Fig. 6 shows the distribution of interlaminar stresses τ_{xz} and σ_z in the laminar plates with stacking sequence $[90^o/0^o]_s$ along x-axis, under the vibration mode for $\varpi_{21} = 274$ rad/s. The results indicate that τ_{xz} arrives at minimum at $x/h = 10$, where σ_z reached the maximum.

Fig. 7 shows the distribution of interlaminar stresses τ_{xz} and τ_{yz} in the laminar plates with stacking

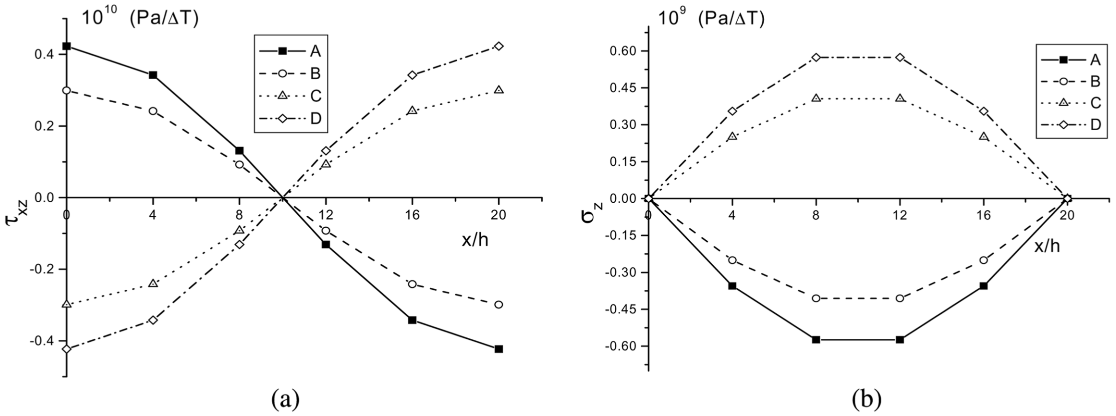

Fig. 6 (a,b) The response histories and distribution of interlaminar stress in laminated plates with the stacking sequence $[90^o/0^o]_s$, under vibration mode of $\varpi_{21} = 274$ rad/s. The curves A, B, C and D represent, respectively, the interlaminar stresses at times $t = 0.5\varpi_{21}\pi$, $t = 0.75\varpi_{21}\pi$, $t = 1.25\varpi_{21}\pi$ and $t = 1.5\varpi_{21}\pi$

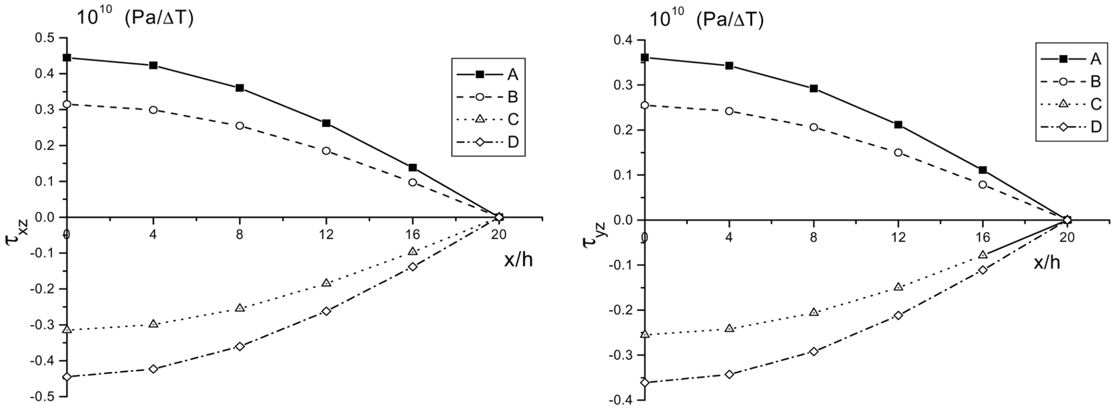

Fig. 7 (a,b) The response histories and distribution of interlaminar stress in laminated plates with the stacking sequence $[45^o/–45^o]_s$, under vibration mode of $\varpi_{11} = 178$ rad/s. The curves A, B, C and D represent, respectively, the interlaminar stresses at times $t = 0.5\varpi_{11}\pi$, $t = 0.75\varpi_{11}\pi$, $t = 1.25\varpi_{11}\pi$ and $t = 1.5\varpi_{11}\pi$

sequence [45°/–45°]$_s$ along x-axis, under the vibration mode for ϖ_{11} = 178 rad/s. The results indicate that both τ_{xz} and τ_{yz} are decreasing along the x-axis. Fig. 8 shows the distribution of interlaminar stresses τ_{xz} and τ_{yz} in the laminar plates with stacking sequence [45°/–45°]$_s$ along x-axis, under the vibration mode for ϖ_{21} = 412 rad/s. The results indicate that both τ_{xz} and τ_{yz} arrive at minimum at x/h = 10.

Fig. 9 shows the distribution of interlaminar stresses τ_{xz} and τ_{yz} at the special position of x = 20 h, y = 20 h, z = h in laminated plates with various layer angles, along x-axis, under the vibration mode for ϖ_{11} = 138 rad/s. The results indicate that both τ_{xz} and τ_{yz} are nearly of the same changing tendency along the x-axis. Thermal load affects the interlaminar stresses most significantly in the laminated plates with stacking sequence [15°/–15°]$_s$ and [45°/–45°]$_s$.

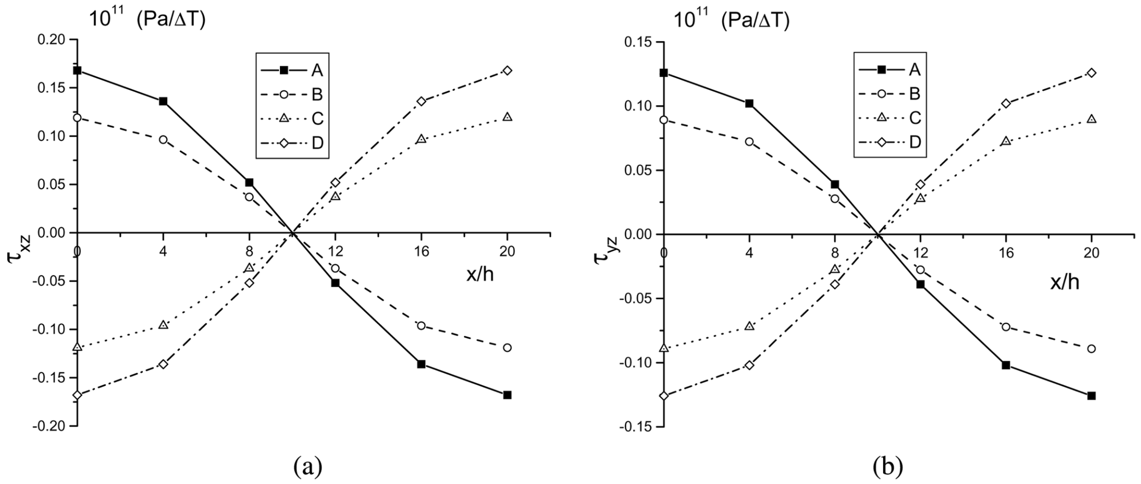

Fig. 8 (a,b) The response histories and distribution of interlaminar stress in laminated plates with the stacking sequence [45°/–45°]$_s$, under vibration mode of ϖ_{21} = 412 rad/s. The curves A, B, C and D represent, respectively, the interlaminar stresses at times $t = 0.5\varpi_{21}\pi$, $t = 0.75\varpi_{21}\pi$, $t = 1.25\varpi_{21}\pi$ and $t = 1.5\varpi_{21}\pi$

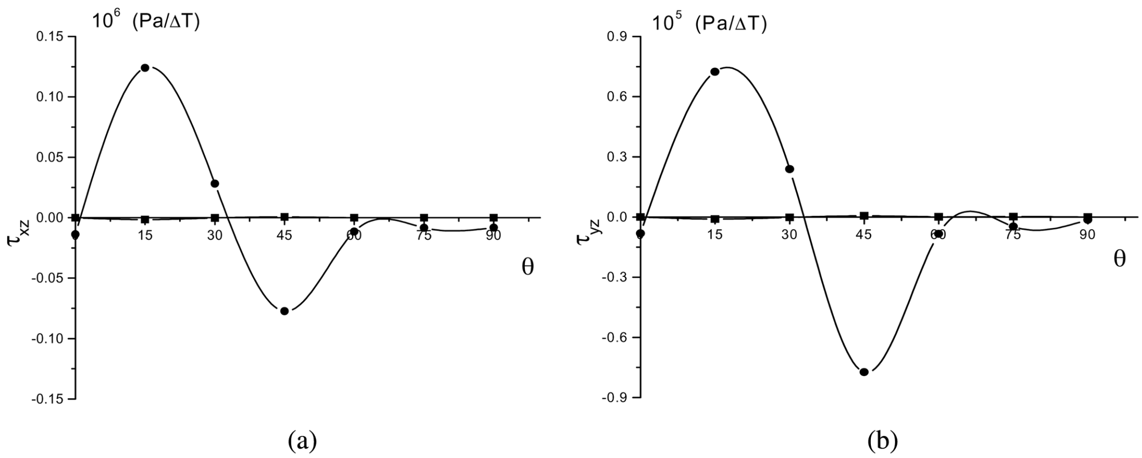

Fig. 9 (a,b) The distributions of interlaminar stresses at x = 20 h, y = 20 h, and z = h_s, with the change of the stacking angle [$\pm\theta$], under the vibration mode of ϖ_{11}

5. Conclusions

In this paper, an analytical method is applied to calculate the response and distribution of dynamic interlaminar stresses in composite laminated plates subjected to free vibration and thermal load. The new features and meaningful numerical results in the present work are given by

1. The maximum interlaminar stresses occur at $t = 0.5\varpi_{mn}\pi$ or $t = 1.5\varpi_{mn}\pi$. The vibration mode also significantly affects the response histories and distribution of interlaminar stresses.
2. Interlaminar stresses vary with the change of plying angle, which are mainly determined by the vibration modes.
3. Thermal load has obviously effect on the dynamic interlaminar stresses at particular position such as the center point of the plane, while has little on other positions. Thermal load affects the response histories and distribution of interlaminar stresses most significantly in the laminated plates with stacking sequence $[15^o/{-15^o}]_s$ and $[45^o/{-45^o}]_s$, so we can design a reasonable stacking sequences to decrease the effect of thermal loading on dynamic interlaminar stresses.

Acknowledgements

The authors thank the referees for their valuable comments.

References

Adams, D.F. and Miller, A.K. (1977), "Hygrothermal microstresses in a unidirectional composite exhibiting inelastic materials behavior", *J. Comput. Mater.*, **11**, 285-299.

Babeshko, M.E. (1996), "Numerical investigation of the plastic stresses-strain state of laminated shells in axisymmetric deformation processes with small-curvature trajectories and allowance for geometric nonlinearity", *Int. Appl. Mech.*, **32**, 646-655.

Bowles, D.E. and Tompkins, S.S. (1989), "Prediction of coefficients of thermal expansion for unidirectional composites", *J. Comput. Mater.*, **23**, 370-381.

Carvalho, A. and Guedes, S.C. (1996), "Dynamic response of rectangular plates of composite materials subjected to impact loads", *Comput. Struct.*, **34**, 55-63.

Cho, M. and Yoon, J.Y. (1999), "Free-edge interlaminar stress analysis of composite laminates by extended Kantorovich method", *AIAA J.*, **37**, 656-660.

Chandrashekhara, K. and Bhimaraddi, A. (1994), Pergamon Press Inc. "Thermal stress analysis of laminated doubly curved shells using a shear flexible finite element", *Comput. Struct.*, **52**, 1023-1030.

Di, S. and Ramm, E.H. (1993), "Hybrid stress formulation for higher-order theory of laminated shell analysis", *Comput. Meth. Appl. Mech. Eng.*, **109**, 359-376.

Ding, K.W. and Tang, L.M. (1999), "Analytical solution of thermal stresses for closed laminated cylindrical shell of arbitrary thickness", *Eng. Mech.*, **16**, 1-5.

Ganapathy, S. and Rao, K.P. (1997), "Interlaminar stresses in laminated composite plates", *Comput. Struct.*, **38**, 157-168.

Jane, K.C. and Hong, C.C. (2000), "Interlaminar stresses of a rectangular laminated plate with simply supported edges subject to free vibration", *Mech. Sci.*, **42**, 2031-2039.

Makeev, A. and Armanios, E.A. (1994), "Simple elasticity solution for predicting interlaminar stresses in laminated composites", *J. Am. Helicopter Soc.*, **44**, 94-100.

Messina, A. and Soldatos, K.P. (2002), "A general vibration model of angle-ply laminated plates that accounts

for the continuity of interlaminar stresses", *Inte. J. Solids Struct.*, **39**, 617-635.
Reddy, J.N. (1996), *Mechanics of Laminated Composite Plates*, London.
Savchenko, V.G. (1995), "Thermal stress state of laminated shells of revolution made of isotropic and linearly orthotropic materials", *Int. Appl. Mech.*, **31**, 249-258.
Tsai, S.W. and Hahn, H.T. (1980), "Introduction to composite materials", Westport, CT: Technomic publishing CO.
Verijenko, V.E. and Tauchert, T.R. (1999), "Refined theory laminated anisotropic shells for thermal stress problems", *J. Therm. Stresses*, **22**, 75-100.
Wilfried, B., Peng, J.P. and Ptra, N. (1999), "Interlaminar stresses at the free corners of a laminate", *Comput. Struct.*, **45**, 155-162.
Yong, Y.K. and Cho, Y. (1995), "Pergamon Press Inc. Higher-order, partial hybrid stress, finite element formulation for laminated plate and shell analyses", *Comput. Struct.*, **57**, 817-827.
Yuan, F.G. (1993), "Thermal stresses in thick laminated composite shells", *Comput. Struct.*, **26**, 63-75.
Ye, J.Q. and Soldatos, K.P. (1996), "Three-dimensional vibration of laminated composite plates and cylindrical panels with arbitrarily located lateral surfaces point supports", *Int. J. Mech. Sci.*, **38**, 271-281.
Zhang, S.Y. and Liu, J.Q. (1992), "Mechanics properties of composite material structures", Beijing Technology University Press.